

Adsorption of Nickel in Aqueous Solution onto Natural Maghnite

Mohamed Amine Zenasni^{1,2,3,*}, Said Benfarhi², André Merlin³, Stéphane Molina³, Béatrice George³, Bahia Meroufel^{1,3}

¹Institute of Sciences and Technology, Department of Sciences, Bechar University, Bechar, Algeria; ²Institute of Sciences, Department of Chemistry, Batna University, Batna, Algeria; ³Laboratory of Studies and Research on Material Wood (LERMAB), University of Lorraine, Nancy, France.

Email: *am.zenasni@gmail.com

Received December 4th, 2012; revised January 1st, 2013; accepted January 5th, 2013

ABSTRACT

Maghnite clay obtained from Tlemcen, Algeria was investigated to remove heavy metal ion from wastewater. Thus, the present study includes the adsorption of Ni(II) in aqueous solution on maghnite clay through the process of adsorption under various conditions (with variable concentration of metal ion, temperature, pH and mixing time). Increasing pH favours the removal of metal ions till they are precipitated as the insoluble hydroxides. The uptake is rapid with maximum adsorption being observed within 10 min for Ni(II). In addition, the results obtained from adsorption isotherm indicated that these data can be better fitted with the Langmuir and Freundlich equations than the Dubinin-Radushkevich (D-R) equation.

Keywords: Natural Maghnite; Ni(II); Adsorption

1. Introduction

The increasing levels of toxic heavy metals or radionuclides, which have been discharged into the environment as industrial wastes, pose a serious threat to human health, living resources and ecological systems. Among the potentially contaminants, nickel is one of the most widespread pollutants in the environment. It is generally regarded that the wastewater containing nickel is mainly derived from industrial production processes including mining, electrolysis, electroplating, batteries dyes metallurgy, pesticides, etc. [1]. ⁶³Ni(II) ($T_{1/2} = 96a$), an important product of the neutron activation of the reactor materials, is present in liquid wastes released from pressurized water from the nuclear power reactors and is also widely used in research and medical applications. The presence of nickel in drinking water above the permissible limit of 0.02 mg/L (WHO drinking-water quality standards) can cause adverse health impacts such as anemia, diarrhea, encephalopathy, hepatitis and the dysfunction of central nervous system. For ecosystem stability and public health sake, it is of great importance to remove nickel from wastewaters. Among most methods of wastewater management, sorption technique has been widely used for the treatment of wastewater and

retention of nuclear waste due to its simplicity of design, high sorption efficiency and low cost. In Sweden, the Svensk Karnbranslehantering AB (SKB, the Swedish Nuclear Fuel and Waste Management Co.) presents an R&D program every three years to manage spent nuclear fuel and other radioactive waste [2]. The studies on the sorption of radionuclides have been extensively conducted. Many R&D programs and various results have been reported [3-8]. For the long-term performance assessment of nuclear waste, it is of great significance to obtain in-depth understanding on the sorption mechanism of radionuclides at solid/water interfaces.

Adsorption reactions of toxic elements onto clay minerals are critical geochemical processes that affect their bioavailability and movement in both soils and sediments. Bentonite (especially maghnite), an expanding 2:1 phyllosilicate clay mineral, is a common component widely distributed in warm and semi-arid temperate regions [9]. Because of its high cation exchange capacity (CEC), swelling properties and large surface area, bentonite is also routinely used as an effective barrier in nuclear waste or hazardous chemical landfills to prevent contamination of groundwater and sub-soils [10-13].

Maghnite is a smectitic clay with a permanent negative structural charge, $\equiv X^-$, generated largely in the octahedral sheet through isomorphous substitution of Al^{3+} with

*Corresponding author.

Mg²⁺, and a smaller variable charge that can be either positive, ≡S-OH₂⁺, or negative, ≡S-O⁻, generated by proton adsorption/desorption reactions at the edges of the mineral. The CEC of bentonite range from 0.70 to 1.30 mole·kg⁻¹, with up to 80% of the exchange capacity derived from the structural charge and the rest from the negative variable charges on the edges of the mineral [14]. The permanent structural charge derived from isomorphous substitution or non-ideal octahedral occupancy can be calculated from a chemical analysis of the clay.

The present study investigates the removal of Ni (II) from aqueous solution using maghnite. The effect of initial heavy metal concentrations was studied and the relationship between pH and removal efficiency was analysed. Experimental results were analysed using the Langmuir, Freundlich and Dubinin-Radushkevich isotherms. The presence of functional groups in the maghnite that may have a role in the sorption process was confirmed by FTIR. The maghnite sample was characterized by scanning electron microscopy (SEM), transmission electron microscopy (TEM) and TG-DTA.

2. Materials and Methods

2.1. Materials

2.1.1. Adsorbent and Characterization

The maghnite used in this work came from a quarry located in Maghnia (North West of Algeria) and was supplied by company "ENOF" (an Algerian manufacture specialized in the production of nonferric products and useful substances). The different chemical elements of the native maghnite were transformed into oxides and analysed by X-ray fluorescence (experiment carried out at ENOF). This maghnite form is stable suspensions in water and had flat platelets or needle-like structures. Granulometry of the crude maghnite have been prepared in the Civil Engineering Department of Tlemcen University (EDTU) in Algeria using a sedimentation technique with a 0.1% solution of sodium hexametaphosphate; 95% of the particles were found to have a diameter of less than 80 μm. The cation exchange capacity was measured to be 101.25 meq/100g of clay, and the surface area was 27 m²/g, with an average pore size of 7 nm.

The Fourier transform infrared (FT-IR) spectra using KBr pressed disk technique were conducted by Perkin Elmer Spectrum 2000 Infrared spectrometer. Natural maghnite and KBr were weighted and then were ground in an agate mortar for 10 min prior to pellet making. The spectrums were collected for each measurement over the spectral range of 400 - 4000 cm⁻¹.

TG-DTA thermograms were plotted using the multi-module 92 - 10 Setaram analyser operating from room temperature up to 1000°C in a Al₂O₃ crucible, at 10°C/mn

heating rate.

Nanomorphology was characterized by scanning electron microscopy (SEM) and transmission electron microscopy (TEM). The SEM study was carried out using Hitachi S-4800 equipped with energy dispersive spectrometry for chemical analysis (EDS) and operating at 15 kV acceleration voltage. TEM study was performed with a Philips CM10 microscope operating at 100 kV.

2.1.2. Adsorbate (Ni²⁺) and Other Chemicals

All chemicals used were of analytical grade. Stock standard solution of Ni²⁺ has been prepared by dissolving the appropriate amount of Ni(NO₃)₂·6H₂O in deionized water, acidified with small amount of nitric acid. This stock solution was then diluted to specified concentrations. The pH of the system was adjusted using reagent grade NaOH and HCl respectively. All plastic sample bottles and glassware were cleaned, then rinsed with deionized water and dried at 60°C in a temperature controlled oven. All measurements were conducted at a room temperature of 20°C. The concentration of Ni²⁺ was measured using Varian 100 Atomic Absorption Spectrophotometer (AAS). The pH of all solution was measured by a TitraLab Instrument TIM800 Model pH meter.

2.2. Adsorption Experiments

2.2.1. Adsorption Procedure

Adsorption measurements were determined by batch experiments. For this purpose, 0.2 g of maghnite and 40 mL of aqueous Ni²⁺ solutions at specified concentration were put on a shaker using a thermostated shaker bath GFL-1083 Model at 20°C for a given time. The suspensions were then centrifuged by Eppendorf 5702 Model digital and these solutions were analyzed using flame atomic absorption spectrophotometer with air-acetylene flame. The pH of the solutions was initially adjusted by addition of small amount of either 0.1 M HCl or 0.1M NaOH solutions. The experiments were carried out by varying concentrations of initial Ni²⁺ solution, contact time, temperature and pH of initial suspension. The Ni²⁺ concentration retained in the adsorbent phase, q_e (mg/g) was calculated according to following relation [15]:

$$q_e = \frac{(C_0 - C_e)V}{m} \quad (1)$$

where C₀ (mg/L) and C_e (mg/L) are the concentration in the solution at time t = 0 and at time t respectively, V is the volume of solution (L) and m is the amount of adsorbent (g) added.

Adsorption percentage (%) was derived from the difference of the initial concentration (C₀, mol/L) and the final one (C_e, mol/L) (Equation (2)):

$$\text{Sorption\%} = \frac{C_0 - C_e}{C_0} \times 100\% \quad (2)$$

2.2.2. Effect of PH

In this study the sorbent (0.2 g) and 20 mL of 100 ppm (mg/L) Ni²⁺ solution were mixed in plastic bottle. The pH of the mixture was adjusted either by 0.1 M HCl or 0.1 M NaOH solution until the initial pH was close to the target value ranged from 2.5 to 7.5. The whole mixture was taken in a series of 50 mL plastic bottles and put on a thermostated shaker bath and at 20°C for a period of 10 min. Speed was such that it maintains the contents completely mixed and the adsorbents were suspended throughout the plastic bottle. The samples were then collected in different time intervals throughout equilibrium time period and centrifuged each time. The left out concentrations in the solution was analyzed using flame atomic absorption spectrophotometer. The quantity of adsorbed metal ion on maghnite was calculated as the difference between initial concentration and concentration at any time, *t* as per (Equation (1)). Each experiment was repeated in twice to check the reproducibility. Measurements are, in general, reproducible within ±10%.

2.2.3. Effect of Temperature

The batch adsorption experiments were carried out with 20 mL Ni(II) metal ion solution of 100 ppm at 20, 30, 40, 50 and 60°C separately by contacting with 0.2 g of adsorbent using thermostated shaker bath for 10 min. The solution pH was 7.5.

2.2.4. Equilibrium Isotherm Experiments

For isotherm studies, a series of 50 mL plastic bottles containing 20 mL of Ni²⁺ metal ions solutions of known concentrations, varying from 10 to 500 mg/L were prepared. Identical amounts (0.2 g) of maghnite were added to the each bottle and the resulting suspensions were agitated on a thermostated shaker bath at 20°C for 10 min at a constant pH of 7.5. After equilibrium time, the suspensions were then centrifuged and the solutions were analyzed using flame atomic absorption spectrophotometer with air-acetylene flame.

3. Results and Discussions

3.1. Characterization of Adsorbent

Chemical analysis data of the natural maghnite are presented in **Table 1**.

These results confirm that the maghnite used consists essentially of montmorillonite, since the ratio SiO₂/Al₂O₃ is equal to 3.77 and thus belongs to the family of the phyllosilicates.

FT-IR studies of these adsorbents help the identification of various forms of the minerals that are present in the clay. Infrared spectra of the charge maghnite, illustrated in **Figure 1**, show the presence of absorption bands of clay phase and absorption characteristic bands of impurities.

A strong band at 3623.90 cm⁻¹ and 3464.43 cm⁻¹ indicates the possibility of the hydroxyl linkage. However, a broad band at 3464.43 cm⁻¹ and a band at 1631.34 cm⁻¹ in the spectrum of clay suggest the possibility of water of hydration in the adsorbent. The bands due to free (or weakly hydrogen-bonded water molecule to the surface oxygen of tetrahedral sheet) water molecules, water-water hydrogen bond (Mⁿ⁺-O-H-O-H-) and water bending modes are observed near 3623.90, 3464.43 and 1631.34 cm⁻¹, respectively. The strong band near 1037.10 cm⁻¹ is due to Si-O-Si stretching vibration in tetrahedral sheets, which corresponds to the characteristic band of montmorillonite [16]. The coupled vibrations are appreciable due to the availability of various constituents. In the IR studies of maghnite, the Si-O stretching vibrations were observed at 697.86 cm⁻¹, 524.86 cm⁻¹ and 469.95 cm⁻¹ showing the presence of quartz. The appearance of ν (Si-O-Si) and δ (Si-O) bands also support the presence of quartz [17]. The vibrations observed at 912.24 cm⁻¹ indicate the possibility of the presence of hematite [18].

Result from thermal analysis is reported in **Figure 2**. The TG curve of the natural maghnite shows three main steps of weight loss. In the first step (T < 200°C) a weight loss (about 18.50%) corresponding to both adsorbed and interlayer water loss takes place. After this step, the TG curve shows a slight gradual decrease (about 2.10%) in the range 200°C - 580°C, which is attributed to the water loss of maghnite. Finally, a third main loss occurs at temperatures in the range 580°C - 900°C, where the TG curve displays a step weight loss (about 4.11%) related to the release of structural OH of natural maghnite. The dehydroxylation temperature of about 650°C (see **Figure 2**) is in agreement with the classical range of dehydroxylation temperature (600°C - 700°C) observed by various authors for cis vacant montmorillonites [19].

SEM micrograph of the untreated maghnite sample suggests a very cohesive material (**Figure 3**). The micro-

Table 1. Chemical composition of the maghnite.

Species	SiO ₂	Al ₂ O ₃	Fe ₂ O ₃	CaO	MgO	Na ₂ O	K ₂ O	TiO ₂	L.O.I [*]
% (w/w)	65.20	17.25	2.10	1.20	3.10	2.15	0.60	0.20	8.20

*L.O.I: Loss on ignition.

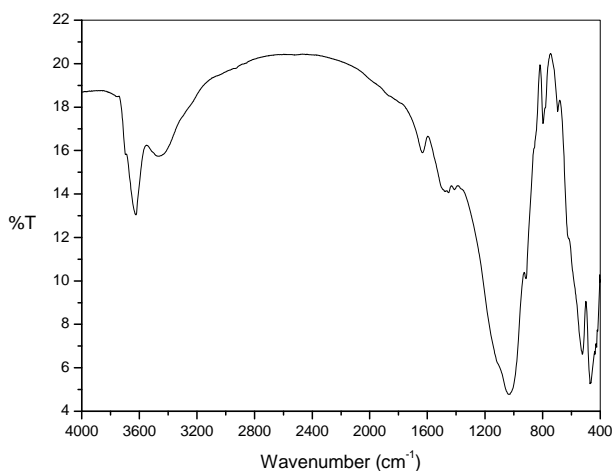


Figure 1. Infrared (IR) spectra of natural maghnite.

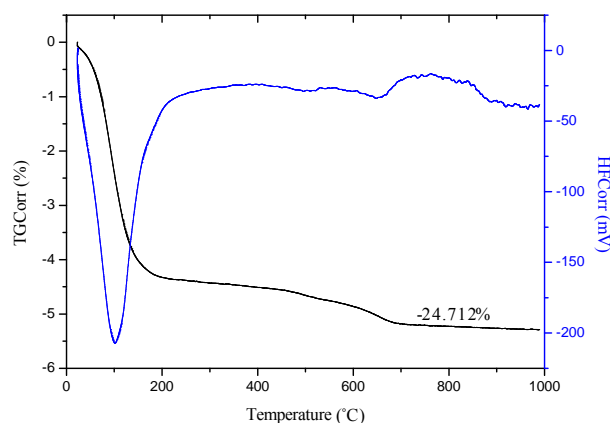


Figure 2. TG-DTA analysis of natural maghnite.

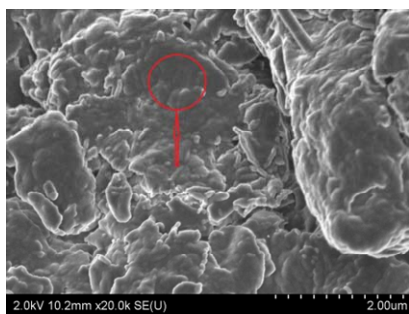


Figure 3. SEM image of maghnite sample.

graph confirms that the material is forming micron-size agglomerates. A higher magnification micrograph of the same structure shows that the micro-size particles are composed of individual platelets, which conglomerate into larger size particles.

The obtained chemical analysis by energy dispersive spectroscopy (Figure 4) shows the presence of framework Al and Si elements. The molar Si/Al ratio for used maghnite is about 2.78. The presence also of the Na, K and Mg elements in the structure of maghnite.

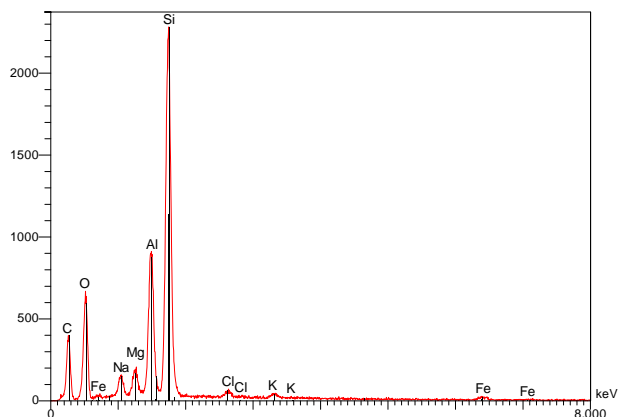


Figure 4. SEM-EDS spectra of maghnite sample.

The TEM micrographs at low magnification showed (Figure 5) a higher tendency of the maghnite to aggregate.

3.2. Effect of Initial Concentration of Ni(II)

Effect of initial concentration of Ni(II) on adsorption capacity of maghnite was investigated by varying initial concentration of Ni(II) from 10 to 500 mg/L. For this study, pH, temperature, adsorbent dosage and contact time have been fixed as 20°C, 0.2 g/20mL and 10 min. The results are presented in Figure 6. An increase of Ni(II) concentration accelerates the diffusion of Ni(II) ions from solution to the adsorbent surface due to the increase in driving force of concentration gradient. Hence, the amount of adsorbed Ni(II) at equilibrium increased from 0.98 to 18.5 mg/g as the Ni(II) concentration is increased from 10 to 500 mg/L.

3.3. Effect of pH

Effect of initial pH on the adsorption capacity of maghnite for Ni(II) was studied by varying solution pH from 2.5 to 7.5 at the adsorbent dosage of 0.2 g/20mL using an initial concentration of Ni(II) as 100 mg/L. The pH range of 2.5 - 7.5 was chosen, as the precipitation of Ni(II) is found to occur at $\text{pH} \geq 8$ [20]. Variation of adsorption capacity of maghnite for Ni(II) ions with pH is shown in Figure 7. It is evident that the adsorption of Ni(II) ions on maghnite is strongly dependant on the pH of the solution. The adsorption of Ni(II) ions increases steadily with increase in initial pH from 2.5 to 7.5 and the maximum adsorption capacity of 9.96 mg/g is observed at pH 7.5.

3.4. Effects of Interaction Time and Kinetics of Adsorption

The adsorption of Ni(II) on maghnite as a function of contact time at $\text{pH} 7.5 \pm 0.1$ is shown in Figure 8.

The Ni(II) interacted with the maghnite rapidly and

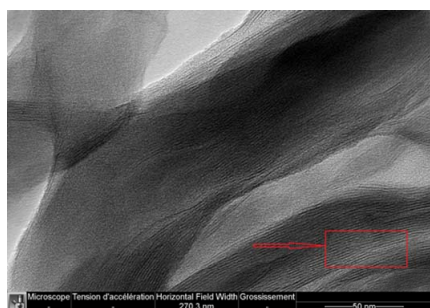


Figure 5. TEM micrograph of the maghnite.

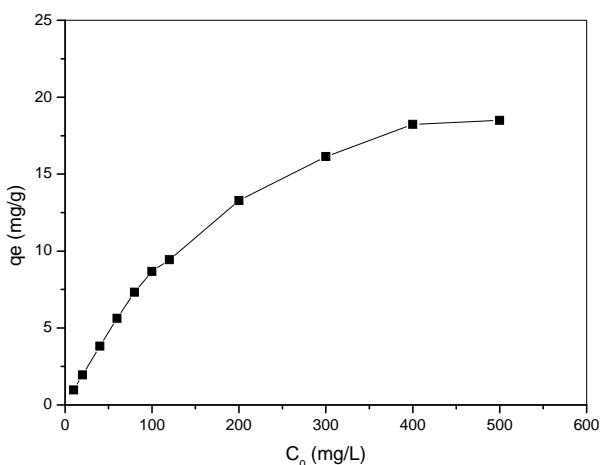


Figure 6. Effect of initial concentration of Ni(II) on adsorption capacity of maghnite.

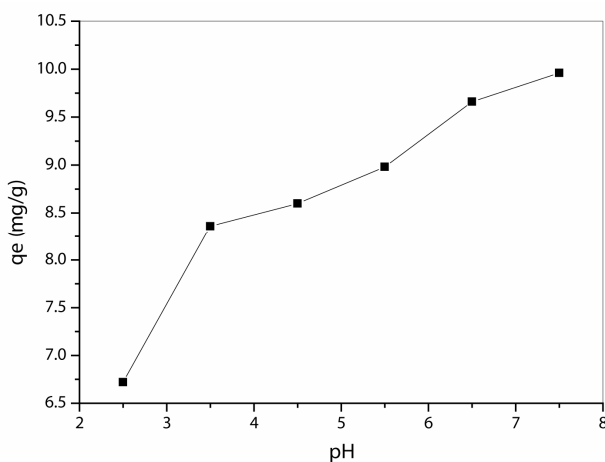


Figure 7. Effect of pH on adsorption capacity of maghnite for Ni(II).

within 6 min, the maximum uptake was observed (Figure 8). Afterwards, the interactions slowed down and approached equilibrium in nearly 10 min under the given set of experimental conditions.

Attainment of equilibrium is influenced by several factors including the nature of the adsorbent and the adsorbate, and the interactions between them.

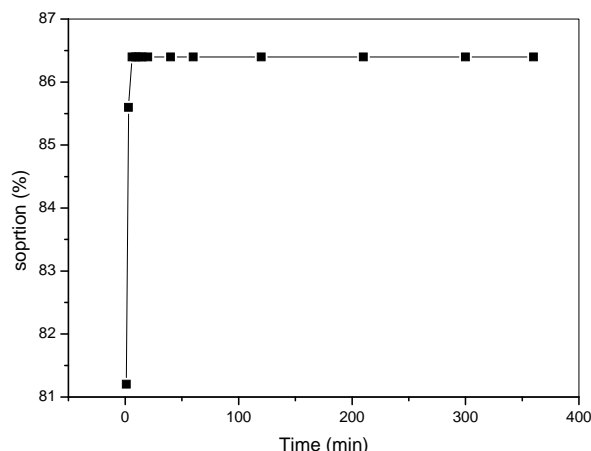


Figure 8. Effect of contact time on the adsorption of Ni(II) to maghnite, pH = 7.5 ± 0.1, T = 293 K, clay 10 g/L, C[Ni(II)]initial = 100 mg/L.

Initially, the rate of adsorption on the bare surface was very high, but as the sites got covered with the Ni(II), the rate decreased. The rate now becomes predominantly dependent on the rate at which metal ions are transported from the bulk liquid phase to the adsorbent-adsorbate interface. The kinetics of the interactions is thus likely to be dependent on different rate processes as the interaction time increases [21].

In this study, 86% of Ni(II), was adsorbed on the maghnite clay when the equilibrium was reached at 10 min. On the basis of this result, it can be observed that natural maghnite clay can be used to remove this metal ion.

The fast adsorption of Ni(II) on maghnite suggested that the uptake of Ni(II) from solution to maghnite was mainly dominated by chemical adsorption rather than physical adsorption [22,23].

To analyze the kinetic adsorption of Ni(II) on maghnite, a pseudo-second-order rate equation was used to simulate the kinetic adsorption (Equation (3)) [24]:

$$\frac{t}{q_t} = \frac{1}{2K'q_e^2} + \frac{1}{q_e}t \quad (3)$$

where q_t (mg/g) is the amount of Ni(II) adsorbed on maghnite at time t (min), q_e (mg/g) is the equilibrium adsorption capacity and K' (g/(mg·min)) is the pseudo-second-order rate constant of adsorption. The values of K' and q_e calculated from the intercept and slope of equation are 5.23 g/(mg·min) and 8.64 mg/g, respectively. The correlation coefficient of the pseudo-second-order rate equation for the linear plot is 1.00 (see Figure 9), which suggests that the kinetic adsorption can be described by the pseudo-second-order rate equation.

3.5. Construction of Isotherms and Model Fitting

Sorption isotherms were constructed by plotting the

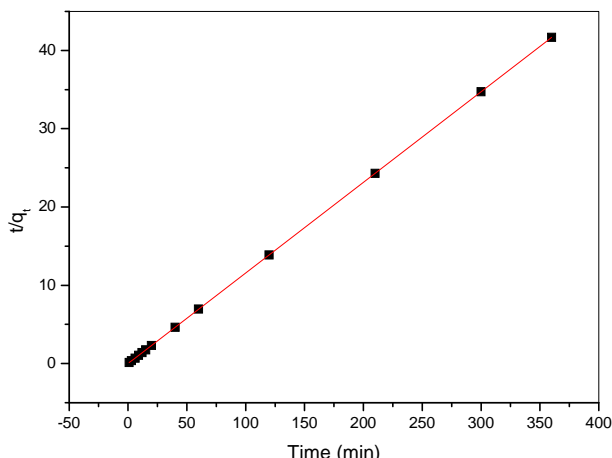


Figure 9. Lagergren pseudo second-order plots for Ni (II) adsorbed on maghnite at 293 K, pH (7.5).

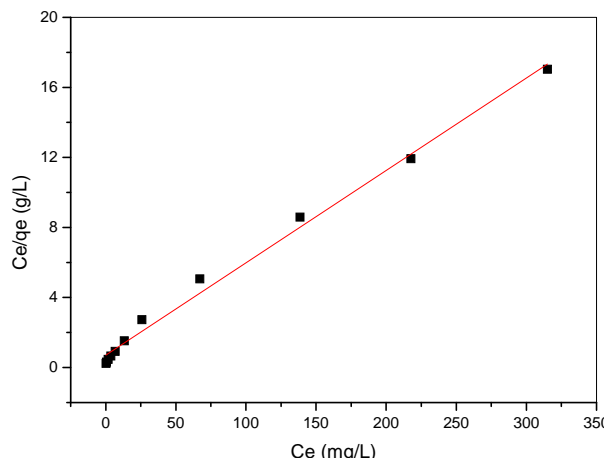


Figure 10. Langmuir isotherm plot for adsorption of Ni²⁺ on the maghnite. *T* = 293 K, initial pH 7.5, *m/V* = 10 g/L.

amount of metal sorbed (mg/g) against the equilibrium concentration of metal in solution (mg/L).

Three models have been adopted in this paper, namely: Langmuir, Freundlich and Dubinin-Radushkevich (D-R) equilibrium isotherm models. The Langmuir and Freundlich isotherms are used most commonly to describe the adsorption characteristics of metal ions in water and wastewater treatment [25].

3.5.1. Langmuir Isotherm

The data conform the linear form of Langmuir model (Equation (4)) [26] expressed below:

$$\frac{C_e}{q_e} = \frac{C_e}{q_m} + \frac{1}{K_L q_m} \tag{4}$$

where *C_e* is equilibrium concentration of Ni(II) (mg/L) and *q_e* is the amount of the Ni²⁺ adsorbed (mg) by per unit of maghnite (g). *q_m* and *K_L* are the Langmuir constants related to the adsorption capacity (mg/g) and the equilibrium constant (L/g), respectively. The Langmuir monolayer adsorption capacity (*q_m*) gives the amount of the metal required to occupy all the available sites per unit mass of the sample (see **Figure 10**). The Langmuir monolayer adsorption capacities of maghnite was estimated as 18.95 mg/g, (**Table 2**). The value of maximum adsorption capacity (*q_m*) calculated from the Langmuir isotherm in this study is much higher than that of those reported in the literature. For example, Langmuir adsorption capacity for Ni(II) adsorption on Oxidized CNTs and As-produced CNTs has been shown to be 9.26 and 18.08 mg/g, respectively, by Kandah and Meunier [27].

3.5.2. Freundlich Isotherm

The adsorption equilibrium data was also applied to the Freundlich model (Equation (5)) [28] given:

$$\log q_e = \log K_f + \left(\frac{1}{n}\right) \log C_e \tag{5}$$

where *K_f* and *n* are Freundlich constants related to adsorption capacity and adsorption intensity, respectively. Freundlich parameters (*K_f* and *n*) indicate whether the nature of adsorption is either favorable or unfavorable. The intercept is an indicator of adsorption capacity and the slope is an indicator of adsorption intensity. A relatively slight slope *n* < 1 indicates that adsorption intensity is good (or favorable) over the entire range of concentrations studied, while a steep slope (*n* > 1) means that adsorption intensity is good (or favorable) at high concentrations but much less at lower concentrations [29]. A high value of the intercept, *K_f*, is indicative of a high adsorption capacity. In the adsorption system, *n* value is 2.63 which indicates that adsorption intensity is good (or favorable) over the entire range of concentrations studied. The *K_f* value of the Freundlich equation (**Table 2**) also indicates that maghnite has a very high adsorption capacity for copper ions in aqueous solutions (see **Figure 11**).

3.5.3. Dubinin-Radushkevich (D-R)

The equilibrium data were also applied to the Dubinin-Radushkevich (D-R) isotherm model to determine if adsorption occurred by physical or chemical processes. The linearized form of the D-R isotherm [30] is as follows (Equation (6)):

$$\ln q_e = \ln q_m - \beta \varepsilon^2 \tag{6}$$

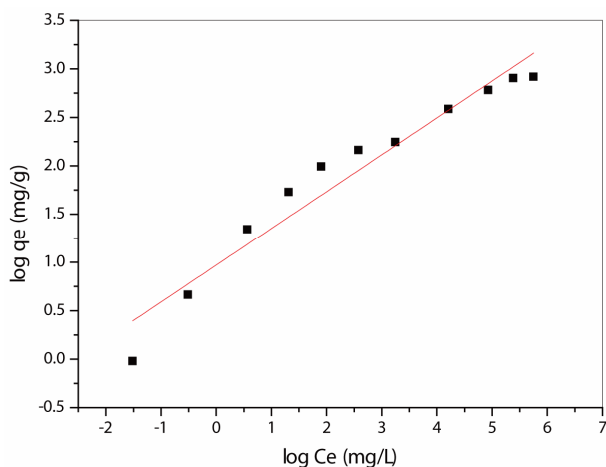
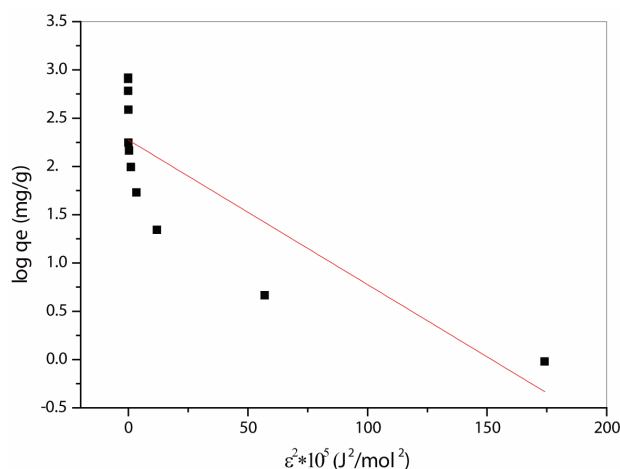
where *β* is the activity coefficient related to mean adsorption energy (mol²/J²) and *ε* is the Polanyi potential (Equation (7)):

$$\varepsilon = RT \ln \left(1 + \frac{1}{C_e} \right) \tag{7}$$

The D-R isotherm is applied to the data obtained from

Table 2. Langmuir, Freundlich and D-R isotherm parameters for the adsorption of Ni²⁺ onto maghnite sample.

Sample	Langmuir isotherm constants			Freundlich isotherm constants			D-R isotherm constants		
Maghnite	q_m (mg/g)	K_L (L/g)	R^2	n	K_f	R^2	q_m (mg/g)	E (kJ/mol)	R^2
	18.95	0.07	0.992	2.63	2.64	0.940	9.71	1.83	0.664

**Figure 11. Freundlich isotherm plot for adsorption of Ni²⁺ on the maghnite. $T = 293$ K, initial pH 7.5, $m/V = 10$ g/L.****Figure 12. D-R isotherm plot for adsorption of Ni²⁺ on the maghnite. $T = 293$ K, initial pH 7.5, $m = 10$ g/L with $R^2 = 0.664$: To demonstrate that this type of adsorption is bad compared the two other.**

the empirical studies. A plot of $\ln q_e$ against ε^2 is given in **Figure 12**. D-R isotherm constants, q_m , for maghnite was found to be 9.71 mg/g (**Table 2**).

The difference of q_m derived from the Langmuir and D-R models is large. The difference may be attributed to the different definition of q_m in the two models. In Langmuir model, q_m represents the maximum adsorption of metal ions at monolayer coverage, whereas it represents the maximum adsorption of metal ions at the total specific micropore volume of the adsorbent in D-R model. Thereby, the value of q_m derived from Langmuir model is higher than that derived from D-R model. The differences are also reported in previous studies [30]. The mean adsorption energy, E (kJ/mol) is as follows (Equation (8)):

$$E = \frac{1}{\sqrt{-2\beta}} \quad (8)$$

This adsorption potential is independent of the temperature, but it varies depending on the nature of adsorbent and adsorbate. The magnitude of E is used for estimating the type of adsorption mechanism. If the E value is between 8 and 16 kJ/mol, the adsorption process follows by chemical adsorption and if $E < 8$ kJ/mol, the adsorption process is of a physical nature [30]. The calculated values of E are 1.83 kJ/mol for maghnite, and they are in the range of values for physical adsorption reactions. The similar results for the adsorption of Ni(II) was reported by earlier worker [29].

3.6. Thermodynamic Studies

Using the following equations, the thermodynamic parameters of the adsorption process were determined from the experimental data (Equations (9)-(11)):

$$\ln K_d = \frac{\Delta S}{R} - \frac{\Delta H}{RT} \quad (9)$$

$$\Delta G = \Delta H - T\Delta S \quad (10)$$

$$K_d = \frac{q_e}{C_e} \quad (11)$$

where K_d is the distribution coefficient for the adsorption, ΔS , ΔH and ΔG are the changes of entropy, enthalpy and the Gibbs energy, T (K) is the temperature, R ($\text{J}\cdot\text{mol}^{-1}\cdot\text{K}^{-1}$) is the gas constant. The enthalpy change (ΔH) is determined graphically by plotting $\ln K_d$ versus $1/T$ which gives a straight line (**Figure 13**) and the values of free energy (ΔG) and entropy (ΔS) computed numerically are presented in **Table 3**.

Free energy values (ΔG) are very small and positive, and decreases with an increase of temperature. This indicates that better adsorption is obtained at higher temperature. The positive values of entropy may be due to some structural changes in the adsorbate and adsorbent during the adsorption process. The positive value of ΔH indicate the endothermic behavior of the adsorption reaction of Ni(II) ions and suggest that a large amount of

Table 3. Thermodynamic parameters for the adsorption of Ni(II) onto maghnite.

Sample	ΔH (kJ/mol)	ΔS (J/mol K)	ΔG (kJ/mol)					R^2
			293 K	303 K	313 K	323 K	333 K	
Maghnite	6.81	17.87	1.57	1.39	1.22	1.04	0.86	0.895

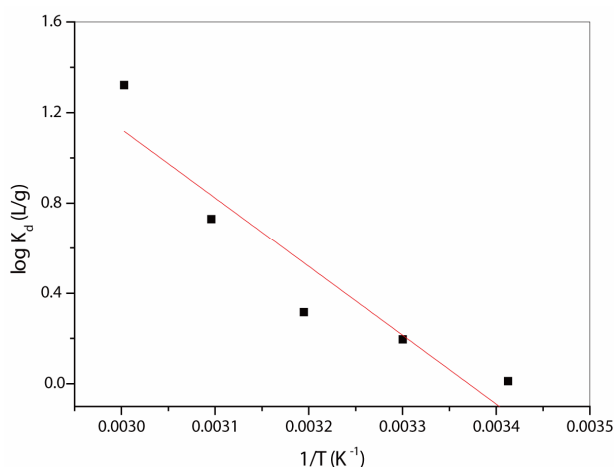


Figure 13. Plot of $\ln K_d$ against $1/T$ for the adsorption of Ni(II) on maghnite, with $R^2 = 0.895$: For this value of R^2 with four temperature value, the results are quite good compared with the literature.

heat is consumed to transfer the Ni(II) ions from aqueous into the solid phase. As was suggested by Nunes and Airoidi [31], the transition metal ions must give up a larger share of their hydration water before they could enter the smaller cavities. Such a release of water from the divalent cations would result in positive value of ΔS . This mechanism of the adsorption of Ni(II) ions is also supported by the positive value of ΔS , which show that Ni(II) ions are less hydrated in the maghnite layers than in the aqueous solution. Also, the positive value of ΔS indicates the increased disorder in the system with changes in the hydration of the adsorbing Ni(II) cations.

4. Conclusion

The present study investigated the performance of the maghnite in removing Ni(II) ions from aqueous solutions. The adsorption of Ni(II) depends upon the nature of the adsorbent surface and the species distribution of Ni(II) in solution, which mainly depends on the pH of the system. The experimental values were evaluated according to the Langmuir, Freundlich and D-R isotherms that are generally used to describe the adsorption processes. The plots have good linearity in both the cases (Freundlich plot, $R^2 = 0.940$, Langmuir plot, $R^2 = 0.992$) at 293 K. Conclusively, the maghnite is a feasible and effective adsorbent in removing Ni(II) ions from aqueous solution.

5. Acknowledgements

The authors gratefully acknowledge to the Dr Yves PILLET (Faculty of Sciences and Technology, group PGCM, University of Lorraine, Nancy, France) because of contribution to our study, and thankful for Joint Service Electronic Microscopy and Microanalysis at the University Henri Poincare of Nancy for MEB-EDS analysis.

REFERENCES

- [1] H. Parab, S. Joshi, N. Shenoy, A. Lali, U. S. Sarma and M. Sudersanan, "Determination of Kinetic and Equilibrium of Co(II), Cr(III), and Ni(II) onto Coir Pith," *Process Biochemistry*, Vol. 41, No. 3, 2006, pp. 609-615. [doi:10.1016/j.procbio.2005.08.006](https://doi.org/10.1016/j.procbio.2005.08.006)
- [2] B. Rosborg and L. Werme, "The Swedish Nuclear Waste Program and the Long-Term Corrosion Behavior of Copper," *Journal of Nuclear Materials*, Vol. 379, No. 1-3, 2008, pp. 142-153. [doi:10.1016/j.jnucmat.2008.06.025](https://doi.org/10.1016/j.jnucmat.2008.06.025)
- [3] D. Cui and T. E. Eriksen, "Reduction of Tc(VII) and Np(V) in Solution by Ferrous Ion. A Laboratory Study of Homogeneous and Heterogeneous Redox Processes," *SKB Technical Report*, 1996.
- [4] F. El Aamrani, I. Casas, J. Pablo, L. Duro, M. Grive and J. Bruno, "Experimental and Modeling Study of the Interaction between Uranium (VI) and Magnetite," *SKB Technical Report*, 1999.
- [5] M. A. Glaus, B. Baeyens, M. Lauber, T. Rabung and L. R. Van Loon, "Water-Extractable Organic Matter from Opalinus Clay: Effect on Sorption and Speciation of Ni(II), Eu(III) and Th(IV)," *Nagra Technical Report*, 2001, pp. 1-7.
- [6] N. Marmier, A. Delisee and F. Fromage, "Surface Complexation Modeling of Yb(III), Ni(II), and Cs(I) Sorption on Magnetite," *Journal of Colloid and Interface Science*, Vol. 211, No. 1, 1999, pp. 54-60. [doi:10.1006/jcis.1998.5968](https://doi.org/10.1006/jcis.1998.5968)
- [7] A. Gustafsson, M. Molera and I. Puigdomenech, "Study of Ni(II) Sorption on Chlorite a Fracture Filling Mineral in Granites, in: Scientific Basis for Nuclear Waste Management XXVIII," *Materials Research Society Symposium Proceedings*, Vol. 824, 2004, pp. 373-378.
- [8] S. Holgersson, "Oskarshamn Site Investigation. Batch Experiments of I, Cs, Sr, Ni, Eu, U and Np Sorption onto Soil from the Laxemar Area," *SKB*, 2009, pp. 9-29.
- [9] R. E. Grim, "Clay Mineralogy," Second Edition, McGraw-Hill Book Co., New York, 1968.
- [10] H. H. Murray, "Traditional and New Application for

- Kaolin, Smectite, and Palygorskite: A General Overview," *Applied Clay Science*, Vol. 17, No. 5-6, 2000, pp. 207-221. [doi:10.1016/S0169-1317\(00\)00016-8](https://doi.org/10.1016/S0169-1317(00)00016-8)
- [11] H. Y. Jo, C. H. Benson and T. B. Edil, "Rate-Limited Cation Exchange in Thin Bentonitic Barrier Layers," *Canadian Geotechnical Journal*, Vol. 43, No. 4, 2006, pp. 370-391. [doi:10.1139/t06-014](https://doi.org/10.1139/t06-014)
- [12] J. Sampler, L. Zheng, L. Montenegro, A. M. Fernandez and P. Rivas, "Coupled Thermo-Hydro-Chemical Models of Compacted Bentonite after FEBEX *in Situ* Test," *Applied Geochemistry*, Vol. 23, No. 5, 2008, pp. 1186-1201. [doi:10.1016/j.apgeochem.2007.11.010](https://doi.org/10.1016/j.apgeochem.2007.11.010)
- [13] A. Harrane, M. A. Belaouedj and M. Belbachir, "Cationic Ring-Opening Polymerization of (d,l-Lactide) Using Maghnite-H⁺, a Non-Toxic Catalyst," *Reactive and Functional Polymers*, Vol. 71, No. 2, 2011, pp. 126-130. [doi:10.1016/j.reactfunctpolym.2010.11.022](https://doi.org/10.1016/j.reactfunctpolym.2010.11.022)
- [14] C. E. Weaver and L. D. Pollard, "The Chemistry of Clay Minerals," Elsevier Science Publishing Company, Oxford, 1975, p. 212.
- [15] S. S. Gupta and K. G. Bhattacharyya, "Immobilization of Pb(II), Cd(II) and Ni(II) Ions on Kaolinite and Montmorillonite Surfaces from Aqueous Medium," *Journal of Environmental Management*, Vol. 87, No. 1, 2008, pp. 46-58. [doi:10.1016/j.jenvman.2007.01.048](https://doi.org/10.1016/j.jenvman.2007.01.048)
- [16] N. Sarier and E. Onder, "Organic Modification of Montmorillonite with Low Molecular Weight Polyethylene Glycols and Its Use in Polyurethane Nanocomposite Foams," *Thermochimica Acta*, Vol. 510, No. 1-2, 2010, pp. 113-121. [doi:10.1016/j.tca.2010.07.004](https://doi.org/10.1016/j.tca.2010.07.004)
- [17] N. Sarier, E. Onder and S. Ersoy, "The Modification of Na-Montmorillonite by Salts of Fatty Acids: An Easy Intercalation Process," *Colloids and Surfaces A: Physicochemical and Engineering Aspects*, Vol. 371, No. 1-3, 2010, pp. 40-49. [doi:10.1016/j.colsurfa.2010.08.061](https://doi.org/10.1016/j.colsurfa.2010.08.061)
- [18] J. D. Desai, H. M. Pathan, S. K. Min, K. D. Jung and O. S. Joo, "FT-IR, XPS and PEC Characterization of Spray Deposited Hematite Thin Films," *Applied Surface Science*, Vol. 252, No. 5, 2005, pp. 1870-1875. [doi:10.1016/j.apsusc.2005.03.135](https://doi.org/10.1016/j.apsusc.2005.03.135)
- [19] A. Leszczynska, J. Njuguna, K. Pielichowski and J. R. Banerjee, "Polymer/Montmorillonite Nanocomposites with Improved Thermal Properties Part II. Thermal Stability of Montmorillonite Nanocomposites Based on Different Polymeric Matrixes," *Thermochimica Acta*, Vol. 454, No. 1, 2007, pp. 1-22.
- [20] O. Abollino, M. Aceto, M. Malandrino, C. Sarzanini and E. Mentasti, "Adsorption of Heavy Metals on Na-Montmorillonite. Effect of pH and Organic Substances," *Water Research*, Vol. 37, No. 7, 2003, pp. 1619-1627. [doi:10.1016/S0043-1354\(02\)00524-9](https://doi.org/10.1016/S0043-1354(02)00524-9)
- [21] S. S. Gupta and K. G. Bhattacharyya, "Immobilization of Pb(II), Cd(II) and Ni(II) Ions on Kaolinite and Montmorillonite Surfaces from Aqueous Medium," *Journal of Environmental Management*, Vol. 87, No. 1, 2008, pp. 46-58. [doi:10.1016/j.jenvman.2007.01.048](https://doi.org/10.1016/j.jenvman.2007.01.048)
- [22] Q. H. Fan, D. D. Shao, J. Hu, W. S. Wu and X. K. Wang, "Comparison of Ni²⁺ Sorption to Bare and ACT-Graft Attapulgites: Effect of pH, Temperature and Foreign Ions," *Surface Science*, Vol. 602, No. 3, 2008, pp. 778-785. [doi:10.1016/j.susc.2007.12.007](https://doi.org/10.1016/j.susc.2007.12.007)
- [23] X. K. Wang, C. L. Chen, W. P. Hu, A. P. Ding, D. Xu and X. Zhou, "Sorption of 243Am(III) to Multiwall Carbon Nanotubes," *Environmental Science & Technology*, Vol. 39, No. 8, 2005, pp. 2856-2860. [doi:10.1021/es048287d](https://doi.org/10.1021/es048287d)
- [24] S.-C. Tsai, S. Ouyang and C.-N. Hsu, "Sorption and Diffusion Behavior of Cs and Sr on Jih-Hsing Bentonite," *Applied Radiation and Isotopes*, Vol. 54, No. 2, 2001, pp. 209-215. [doi:10.1016/S0969-8043\(00\)00292-X](https://doi.org/10.1016/S0969-8043(00)00292-X)
- [25] K. G. Bhattacharyya and S. S. Gupta, "Kaolinite and Montmorillonite as Adsorbents for Fe(III), Co(II) and Ni(II) in Aqueous Medium," *Applied Clay Science*, Vol. 41, No. 1-2, 2008, pp. 1-9. [doi:10.1016/j.clay.2007.09.005](https://doi.org/10.1016/j.clay.2007.09.005)
- [26] I. Langmuir, "The Adsorption of Gases on Plane Surfaces of Glass, Mica and Platinum," *Journal of American Society*, Vol. 40, No. 9, 1918, pp. 1361-1403. [doi:10.1021/ja02242a004](https://doi.org/10.1021/ja02242a004)
- [27] M. I. Kandah and J.-L. Meunier, "Removal of Nickel Ions from Water by Multi-Walled Carbon Nanotubes," *Journal of Hazardous Materials*, Vol. 146, No. 1-2, 2007, pp. 283-288. [doi:10.1016/j.jhazmat.2006.12.019](https://doi.org/10.1016/j.jhazmat.2006.12.019)
- [28] H. Freundlich, "Über die Adsorption in Lösungen," *Zeitschrift für Physikalische Chemie (Leipzig)*, Vol. 57, 1906, pp. 385-470.
- [29] R. Al Dwairi and A. Al-Rawajfeh, "Removal of Cobalt and Nickel from Wastewater by Using Jordan Low-Cost Zeolite and Bentonite," *Journal of the University of Chemical Technology and Metallurgy*, Vol. 41, No. 1, 2012, pp. 69-76.
- [30] D. Xu, X. L. Tan, C. L. Chen and X. K. Wang, "Adsorption of Pb(II) from Aqueous Solution to MX-80 Bentonite: Effect of pH, Ionic Strength, Foreign Ions and Temperature," *Applied Clay Science*, Vol. 41, No. 1-2, 2008, pp. 37-46. [doi:10.1016/j.clay.2007.09.004](https://doi.org/10.1016/j.clay.2007.09.004)
- [31] E. Eren, "Removal of Copper Ions by Modified Unye Clay, Turkey," *Journal of Hazardous Materials*, Vol. 159, No. 2-3, 2008, pp. 235-244. [doi:10.1016/j.jhazmat.2008.02.035](https://doi.org/10.1016/j.jhazmat.2008.02.035)